Communications in Transportation Research 5 (2025) 100190

Contents lists available at ScienceDirect

Communications in Transportation Research

journal homepage: www.journals.elsevier.com/communications-in-transportation-research

Full Length Article

Situational awareness using set-based estimation and vehicular communication: An occluded pedestrian-crossing scenario

Vandana Narri [a,b,*], Amr Alanwar [c], Jonas Mårtensson [b], Henrik Pettersson [a], Fredrik Nordin [a], Karl Henrik Johansson [b]

[a] Autonomous Transport Systems, Research and Development, Scania CV AB, Sodertalje, 151 87, Sweden
[b] School of Electrical Engineering and Computer Science, KTH Royal Institute of Technology, Stockholm, 114 28, Sweden
[c] School of Computation, Information and Technology, Technical University of Munich, Heilbronn, 74076, Germany

ARTICLE INFO

Keywords:
Set-based estimation
Safety guarantees
Vehicle-to-everything (V2X) communication
Shared situational awareness

ABSTRACT

The safety of unprotected road-users is crucial in any urban traffic. Occlusions and blind spots in the field-of-view of a vehicle can lead to unsafe situations. In this work, a specific pedestrian-crossing scenario is considered with an occlusion in the ego-vehicle's field-of-view. A novel framework is presented to enhance situational awareness based on vehicle-to-everything (V2X) communication to share perception data between vehicle and roadside units. It leverages set-based estimation utilizing a computationally efficient algorithm, for which the pedestrian is guaranteed to be located in a constrained zonotope. The proposed method has been validated through both simulation and real experiments. The real experiments are carried out on a test track using Scania autonomous vehicles.

1. Introduction

The development of connected and automated vehicles (CAVs) has progressed rapidly over the past couple of decades. This, in turn, has increased the complexity of CAVs in terms of their number of hardware and software components. The standard ISO 21448:2022 emphasizes functional safety and mitigating risks due to unexpected operating conditions for CAV systems, see ISO (2022). A system state is considered safe if it can guarantee collision avoidance despite of various uncertain urban scenarios. Stefan et al. (2020) highlighted that scenario-based testing plays a key role in CAV safety validation. A scenario is defined as a sequence of events and actions that describes the development between scenes, as stated in Simon et al. (2015) and Graebener (2024). To ensure the safe operation of a CAV, it is necessary to show that it can handle a series of complex scenarios.

This study considers an occluded pedestrian-crossing scenario. The initial scene of the scenario is presented in Fig. 1, with G_x and G_y highlighting the global coordinates of the scene. The ego-vehicle is moving towards the pedestrian crossing, but the sidewalk is occluded by a parked vehicle. This leads to an unsafe situation for the pedestrian in the occluded region. To mitigate the risk of such potential situations, our strategy is to leverage vehicle-to-everything (V2X) communication between the ego-vehicle and sensor units nearby.

1.1. Contributions

The main contribution of this study is a situational awareness framework evaluated on the occluded pedestrian-crossing scenario. In order to provide safety guarantees, we propose to use set-based estimation and fusion, which computes all possible states of the detected pedestrian, allowing the ego-vehicle to determine if any of them intersect with the ego-vehicle's planned path. The set-based algorithm comprises two components.

1) The set-based estimation computes a set that contains the true location of the detected pedestrian.
2) The set-based fusion integrates multiple estimated sets for a detected pedestrian.

Together, these components provide robust safety guarantees for the detected pedestrian. The approach is evaluated in realistic simulations as well as in real experiments. The influence of V2X connectivity between road and users is studied in detail. It is shown how onboard sensors and external sensors via V2X communication effectively

* Corresponding author. Autonomous Transport Systems, Research and Development, Scania CV AB, Sodertalje, 151 87, Sweden.
E-mail address: narri@kth.se (V. Narri).

https://doi.org/10.1016/j.commtr.2025.100190
Received 26 November 2024; Received in revised form 25 January 2025; Accepted 4 February 2025
Available online 11 June 2025

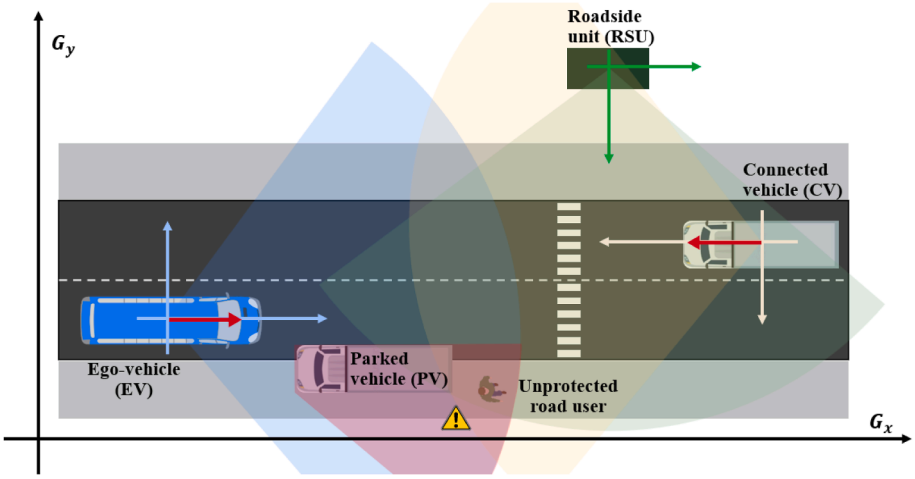

Fig. 1. Considered occluded pedestrian-crossing scenario consists of five actors: ego-vehicle, roadside unit, connected vehicle, parked vehicle, and pedestrian (unprotected road-user). The pedestrian is in the occlusion created by the parked vehicle in the ego-vehicle's field-of-view.

compensate for uncertainties in measurements and system model.

1.2. Literature review

There are many recent research contributions on utilizing V2X communication to improve ego-vehicle situational awareness. Hieu et al. (2023) and Ryan et al. (2018) emphasized that one way is to create collaborative perception is by sharing object detections and using neural networks to fuse the data. Zhu et al. (2024) proposed an alternative method that only requires to share object detection in the region of interest. Han et al. (2023) listed a detailed survey of existing collaborative perception methods using vehicular communication, datasets, and challenges of incorporating collaborative perception in traffic scenarios. They highlighted real-world issues, such as communication imperfections and delays, localization errors, model discrepancies, and security issues, which each one can deteriorate the system's safety. The importance of security and testing is discussed by Jian et al. (2019), Monowar et al. (2020), and Olovsson et al. (2022).

In the absence of V2X communication, van der Ploeg et al. (2024) suggested an approach to handling occluded scenarios through occlusion-aware planning. They proposed a planner that incorporates seen objects and reachable sets of possible hidden objects of arbitrary shape and size. While implementing such a planner is helpful, it remains highly uncertain about the surroundings and requires significant computational power. Sánchez et al. (2022) proposed a framework to reduce the number of hidden object in occluded scenario by sequential reasoning based on reachability analysis and pervious on-board sensor observations. This approach is effective but has a high likelihood of becoming too conserved. This framework is then extended by using V2X communication in (Nyberg et al., 2024). Gilroy et al. (2021) provided a detailed overview of occlusion handling methods. Leveraging V2X communication to share information can help reduce uncertainty regarding road-users in occluded regions.

Wang and Wu (2021) highlighted that uncertainty in scenarios with limited information has a negative impact on the performance of transportation systems. Autonomous driving requires safety guarantees. Safety guarantees can be characterized by robust set-based estimators (Rego et al., 2018). Alanwar et al. (2023) showcased how such estimators compute the set of states consistent with the model and the set consistent with the measurements to obtain the so-called corrected state set. Many researchers have considered set-based estimation for self-localization of autonomous robots (Marco et al., 2003), drones (Merhy et al., 2020), and other vehicles (Althoff, 2010; Bento et al., 2019). Rohou et al. (2017) have showed that the method is particularly advantageous in dynamic and unknown environments.

Set-based estimators have also been used in fault detection (Puig, 2010), underwater robotics (Jaulin, 2009), ground vehicles (Franzè and Lucia, 2015), multi-agent systems (García et al., 2020), and localization (Bouron et al., 2001). There are various ways to mathematically represent the estimated sets, for example, ellipsoids (Merhy et al., 2020), zonotopes (Alanwar et al., 2023), polytopes (Blesa et al., 2012), orthotopes (Hamdi et al., 2016), and intervals (Feng et al., 2020). Constrained zonotopes provide a set representation that combines the flexibility of convex polytopes with the efficiency and scalability of zonotopes, as highlighted by Scott et al. (2016). In this study, the fused sets are represented by constrained zonotopes. Due to their computational properties, the algorithms can run onboard the ego-vehicle.

1.3. Outline

The structure of the remaining paper is briefly described. Section 2 details the problem formulation and the considered scenario. Section 3 gives preliminaries on constrained zonotopes. The proposed framework and algorithm are described in Section 4. In Section 5, results from the simulation test are presented and followed by the real experiments in Section 6. Finally, we conclude the study in Section 7.

2. Problem formulation

In this section, the occluded pedestrian-crossing scenario is described together with the problem statement.

2.1. Scenario description

The pedestrian-crossing scenario is presented in Fig. 1. It consists of five actors: an ego-vehicle (EV), a roadside unit (RSU), a connected vehicle (CV), a parked vehicle (PV), and a pedestrian. The EV, RSU, and CV have the ability to communicate with each other through their V2X units. The EV moves from left to right. The PV is creating an occlusion in the EV's field-of-view (FOV), which is indicated by the red area. The CV moves from right to left. The RSU is a stationary unit positioned in a way that covers the pedestrian-crossing. An unsafe set in the scenario is a set of states in $\mathbb{R}^2$ that contains both the predicted state of the pedestrian and the reachable state of the EV. The measurement of a pedestrian at time t is assumed to be a set $\mathcal{M}_t \subset \mathbb{R}^2$. This set is consistent with the true location of the pedestrian in the EV coordinate frame. Depending on the specific scenario, measurement sets are provided by the EV, RSU, and CV, when the pedestrian is present in their FOV. If the pedestrian is not detected, then $\mathcal{M}_t$ is an empty set.

2.2. Problem statement

In the considered scenario, the pedestrian is moving towards the crossing. The EV is approaching the crossing and is not detecting the pedestrian because of the PV occlusion. If the EV does not detect the pedestrian within a sufficient amount of time to plan and execute a safe maneuver, it might lead to a collision. The problem considered in this study is to develop an algorithm to provide safety guarantees by improving situational awareness for the EV when it faces a scenario with occlusion. The EV can receive measurements from the RSU and CV. It is assumed that there are no false detections from any of the V2X units. Each unit has the capability to provide a measurement set $\mathcal{M}_t^i$ for the detected road-user in its FOV at time t with $i = 1, \ldots, n$, where n is the total number of units. The aim is to estimate set of reachable states for the pedestrian.

3. Preliminaries

To perform set-based estimation and fusion, we utilize hyperplanes, strips, convex polytopes, and constrained zonotopes. These sets and some operations are defined in this section.

A hyperplane $\mathcal{H} \in \mathbb{R}^\gamma$ for some $\gamma > 1$ is a set which is given by

$$\mathcal{H} = \{x \in \mathbb{R}^\gamma | h^T x = b\} \tag{1}$$

where $h \in \mathbb{R}^\gamma$ is a column vector and $b \in \mathbb{R}$ is a scalar. A halfspace is a set of form $\{x \in \mathbb{R}^\gamma | h^T x \leq b\}$. A hyperplane thus divides $\mathbb{R}^\gamma$ into two halfspaces. This mathematical representation of a set is called H-representation, as stated by Althoff (2010). A strip is given by

$$\mathcal{S} = \{x \in \mathbb{R}^\gamma | |h^T x - y| \leq r\} \tag{2}$$

where $y \in \mathbb{R}$ and $r > 0$ are scalars. It is the intersection of two halfspaces with parallel bounding hyperplanes. The intersection of two or more strips can result in a convex polytope, see Fig. 2. Any bounded convex polytope $\mathcal{V}$ can be represented as the intersection of $m \geq \gamma$ strips: $\mathcal{V} = \bigcap_{i=0}^{m} \mathcal{S}_i$.

A constrained zonotope $\mathcal{C} \subset \mathbb{R}^\gamma$ (Scott et al., 2016) is a special type of bounded convex polytope:

$$\mathcal{C} = \{x \in \mathbb{R}^\gamma | x = c + G\beta, A\beta = b, \ \|\beta\|_\infty \leq 1\} \tag{3}$$

where $c \in \mathbb{R}^\gamma$ is the center and $G = [g_1, \ldots, g_e] \in \mathbb{R}^{\gamma \times e}$, $e > 0$, is the generator matrix of the zonotope. The matrix $A \in \mathbb{R}^{\gamma_c \times e}$, $\gamma_c > 0$, and the vector $b \in \mathbb{R}^{\gamma_c}$ define the constraints. $\beta \in \mathbb{R}^e$ is called the scaling factor and $\|\beta\|_\infty = \max_{i=1,\ldots,e} |\beta_i|$. The shorthand notation of a constrained zonotope is $\mathcal{C} = \langle c, G, A, b \rangle$. This way of representing constrained zonotopes using generators is called CG-representation, as stated by Scott et al. (2016).

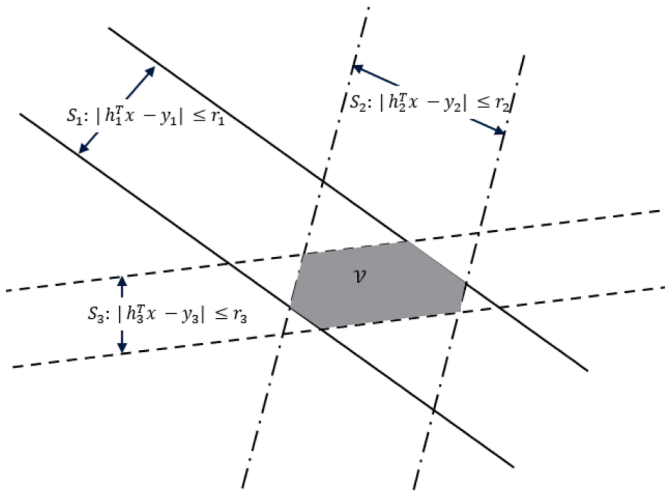

Fig. 2. Illustration of the intersection of three strips $\mathcal{S}_1, \mathcal{S}_2$, and $\mathcal{S}_3$, resulting in the convex polytope $\mathcal{V}$.

Given two constrained zonotopes $\mathcal{C}_1 = \langle c_1, G_1, A_1, b_1 \rangle$ and $\mathcal{C}_2 = \langle c_2, G_2, A_2, b_2 \rangle$, the Minkowski sum is

$$\mathcal{C}_1 \oplus \mathcal{C}_2 = \langle c_1 + c_2, [G_1 \quad G_2], \begin{bmatrix} A_1 & 0 \\ 0 & A_2 \end{bmatrix}, \begin{bmatrix} b_1 \\ b_2 \end{bmatrix} \rangle$$

The computation complexity of the Minkowski sum is $\mathcal{O}(\gamma)$ (Scott et al., 2016). A linear mapping of a constrained zonotope is defined as

$$M\mathcal{C}_1 = \langle Mc_1, MG_1, A_1, b_1 \rangle$$

where $M \in \mathbb{R}^{m \times \gamma}$. The computational complexity of the linear map is $\mathcal{O}(m\gamma e)$ (Scott et al., 2016).

4. Methodology

In this section, the shared situational awareness framework is presented, followed by a description of the estimation–fusion algorithm.

4.1. Architecture

The proposed architecture consists of three types of modules: sensor, estimator, and fusion center, as shown in Fig. 3. There are n sensors corresponding to the V2X units in a given scenario. Sensor i produces a measurement set $\mathcal{M}_t^i$ at time t of the pedestrian in its FOV.

The measurement sets are then inputs to their respective estimator. Each estimator i computes an estimated set $\overline{\mathcal{C}}_t^i$ for the detected pedestrian using the previously estimated set at time $t-1$ and measurement set $\mathcal{M}_t^i$. The estimated sets are then fused in the fusion center. The fused set is denoted by $\mathcal{C}_t$ and is guaranteed that it contains the location of the detected pedestrian.

4.2. Algorithm

We perform the set-based computations using constrained zonotopes because they lead to an algorithm with low computational complexity compared to other set representations. The set-based estimation and fusion algorithm is illustrated in Fig. 4.

4.2.1. Set-based estimation

The estimators take as their input measurement sets obtained from sensors. We omit the superscript i that indicates sensor i, $i = 1, \ldots, n$. A sensor measurement at time t is a set $\mathcal{M}_t \subset \mathbb{R}^2$. It is assumed to be the intersection of strips:

$$\mathcal{M}_t = \{x_t \in \mathbb{R}^2 | |h_t^{\ell T} x_t - y_t^\ell| \leq r_t^\ell, \ell = 1, 2\} \tag{4}$$

We denote such a measurement set as $\mathcal{M}_t = \langle H_t, y_t, R_t \rangle$:

$$H_t = \begin{bmatrix} h_t^1 & h_t^2 \end{bmatrix}, y_t = \begin{bmatrix} y_t^1 \\ y_t^2 \end{bmatrix}, R_t = \begin{bmatrix} r_t^1 & 0 \\ 0 & r_t^2 \end{bmatrix}$$

The set-based estimator computes a set that is guaranteed to contain the location of the pedestrian. A discrete-time linear system is considered to model the motion of the pedestrian:

$$x_t = F_t x_{t-1} + z_t \tag{5}$$

where $x_t \in \mathbb{R}^2$ is the location of the pedestrian, $F_t \in \mathbb{R}^{2 \times 2}$ the transition matrix, and $z_t \in \mathbb{R}^2$ the uncertainty of the pedestrian velocity and heading. The unknown initial position of the pedestrian is denoted x_0 and assumed to be bounded by an initial estimated set $\overline{\mathcal{C}}_0 \subset \mathbb{R}^2$. The uncertainties in the motion model are represented by a constrained

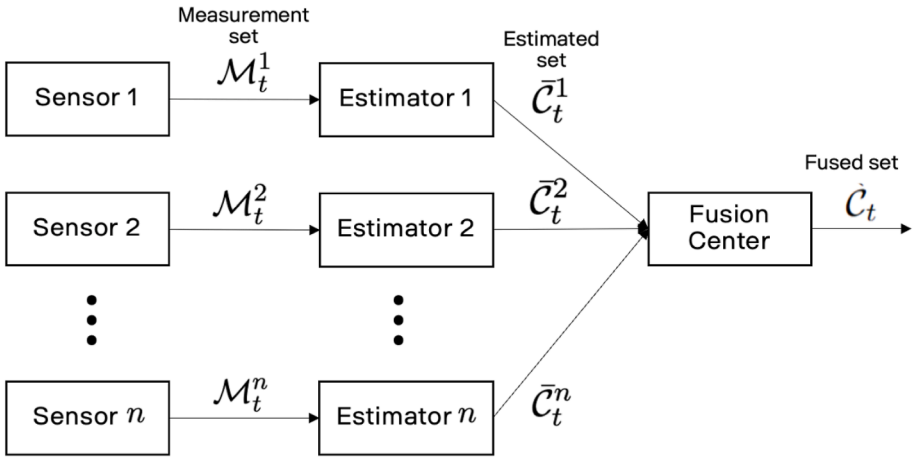

Fig. 3. Architecture of the proposed shared situational awareness framework. The fused set $\mathscr{C}_t$ for the pedestrian is computed using the measurement sets $\mathscr{M}_t^i, i = 1, \ldots, n$, filtered through a bank of estimators and a fusion center.

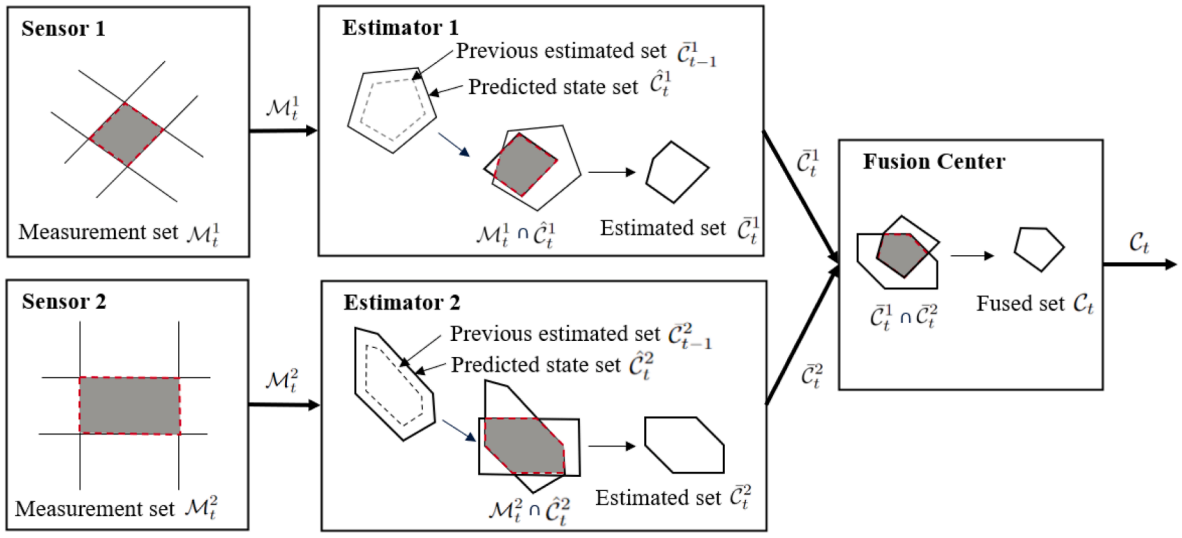

Fig. 4. Illustration of the set-based computations in the estimators and the fusion center for a setup with two sensors.

zonotope: $z_t \in \mathscr{C}_{Q,t} = \langle 0, Q_t, 0, 0 \rangle$ with $Q_t = \text{diag}([q_t^1, q_t^2])$. Let us describe how the estimated set $\overline{\mathscr{C}}_t$ is obtained, see Fig. 4. The predicted state set $\widehat{\mathscr{C}}_t \subset \mathbb{R}^2$ is computed as

$$\widehat{\mathscr{C}}_t = F_t \overline{\mathscr{C}}_{t-1} \oplus \mathscr{C}_{Q,t} \tag{6}$$

Based on this, the new estimated set is given by

$$\overline{\mathscr{C}}_t = \widehat{\mathscr{C}}_t \cap \mathscr{M}_t \tag{7}$$

Note that the resultant estimated set $\overline{\mathscr{C}}_t$ is a constrained zonotope. The set-based estimation algorithm is the first half of Algorithm 1. From line 5, to compute predicted set, we perform linear map and minkowski sum. Since we consider $\gamma = 2$, the worst-case computational complexity can be written as $\mathscr{O}(2^2 e + 2) = \mathscr{O}(e)$, where e is the number of generators of the constrained zonotope. If there exists a measurement set $\mathscr{M}_t$, lines 7–9 involve some low order operations and two matrix multiplication. The worst-case computational complexity of these lines is bounded by $\mathscr{O}(2^2 e + \gamma_c e)$, where γ_c is the number of constraints of the constrained zonotope. If a measurement set does not exist, then there is no computation required. We simply use the predicted set as shown in line 11 in Algorithm 1. Based on this, the worst-case computational complexity for the set-based estimation is bounded by $\mathscr{O}(\gamma_c e + e) = \mathscr{O}(\gamma_c e)$ for each sensor. This is also verified experimentally in Section 6.

Algorithm 1. Set-based estimation and fusion

1: **Input:** $\overline{\mathscr{C}}_0^i, \mathscr{C}_{Q,t}^i, \mathscr{M}_t^i, i = 1, \ldots, n$
2: **Output:** $\mathscr{C}_t$
3: **for** time step $t = 1, 2, \ldots$ **do**
4: **for** sensor $i = 1, \ldots, n$ **do**
5: $\widehat{\mathscr{C}}_t^i := \langle \widehat{c}_t^i, \widehat{G}_t^i, \widehat{A}_t^i, \widehat{b}_t^i \rangle = F_t \overline{\mathscr{C}}_{t-1}^i \oplus \mathscr{C}_{Q,t}^i$.
6: **if** Measurement set $\mathscr{M}_t^i := \langle H_t^i, y_t^i, R_t^i \rangle$ exists **then**
7: $\overline{\mathscr{C}}_t^i := \langle \overline{c}_t^i, \overline{G}_t^i, \overline{A}_t^i, \overline{b}_t^i \rangle$,
8: $\overline{c}_t^i := \widehat{c}_t^i$, $\overline{G}_t^i := \begin{bmatrix} \widehat{G}_t^i & 0 \end{bmatrix}$,
9: $\overline{A}_t^i := \begin{bmatrix} \widehat{A}_t^i & 0 \\ H_t^i \widehat{G}_t^i & -R_t^i \end{bmatrix}$, $\overline{b}_t^i := \begin{bmatrix} \widehat{b}_t^i \\ y_t^i - H_t^i \widehat{c}_t^i \end{bmatrix}$
10: **else**
11: $\overline{\mathscr{C}}_t^i := \widehat{\mathscr{C}}_t^i$
12: **end if**
13: **end for**
14: $\mathscr{C}_t := \langle c_t, G_t, A_t, b_t \rangle$
15: $c_t := \overline{c}_t^1$, $G_t := \begin{bmatrix} \overline{G}_t^1 & 0 & \ldots & 0 \end{bmatrix}$,

(*continued on next page*)

(*continued*)

16: $A_t := \begin{bmatrix} \overline{A}_t^1 & 0 & \dots & 0 \\ 0 & \overline{A}_t^2 & \dots & 0 \\ \vdots & \vdots & \ddots & \vdots \\ 0 & 0 & \dots & \overline{A}_t^n \\ \overline{G}_t^1 & -\overline{G}_t^2 & \dots & 0 \\ \vdots & \vdots & \ddots & \vdots \\ \overline{G}_t^1 & 0 & \dots & -\overline{G}_t^n \end{bmatrix}, b_t := \begin{bmatrix} \overline{b}_t^1 \\ \overline{b}_t^2 \\ \vdots \\ \overline{b}_t^n \\ \overline{c}_t^2 - \overline{c}_t^1 \\ \vdots \\ \overline{c}_t^n - \overline{c}_t^1 \end{bmatrix}$

17: **end for**

There are two cases when the measurement set is not used in the update Eq. (7). First, when a sensor fails to provide a measurement set. Second, when there is a false detection that can lead to an empty measurement set. The convergence of set-based estimation depends on the consistency of the measurement sets and uncertainty bounds in the motion model of the pedestrian.

4.2.2. Set-based fusion

Given the estimated sets $\overline{\mathscr{C}}_t^i$, $i = 1, \dots, n$, the output of the fusion center $\mathscr{C}_t$ is their intersection:

$$\mathscr{C}_t = \overline{\mathscr{C}}_t^1 \cap \dots \cap \overline{\mathscr{C}}_t^n \tag{8}$$

Equation (7) constrained zonotope. The set-based fusion algorithm is the second half of Algorithm 1. From line 14 to line 16, the computational complexity for set-based fusion can be written as $\mathscr{O}(\gamma_{c1}e_1 + \gamma_{c2}e_2 + \dots + \gamma_{cn}e_n)$. For the worst-case, this computational complexity can be generalized as $\mathscr{O}(n\gamma_c e)$. This is also verified experimentally in Section 6. Note that the presented algorithm assumes that measurement sets are non-empty and consistent. If it anyhow happens that $\mathscr{C}_t$ becomes an empty set, it means that the measurement sets are not consistent. Such a situation could be due to faults or the detection of multiple pedestrians. This case is not considered in this study, but will be studied in future work, see Section 7.

Both estimation and fusion steps experience increased computational complexity as the complexity of the constrained zonotope grows. During these steps, the number of zonotope constraints and generators can increase rapidly. To manage the computational complexity of the algorithm, the complexity of a constrained zonotope can be reduced periodically by lowering γ_c and e. Scott et al. (2016) proposed a three-step method to reduce complexity of a constrained zonotope: rescale, reduce γ_c, and e. According to Scott et al. (2016), the computational complexity to rescale is $\mathscr{O}(\gamma_c e^2)$. The computational complexity to reduce γ_c is $\mathscr{O}((e + \gamma_c)^3)$. Finally, the computational complexity to reduce k generators from $G \in \mathbb{R}^{2\times e}$ is $\mathscr{O}(2^2 e + 2ke)$.

5. Simulation results

This section presents simulation evaluations of the proposed framework. The occluded pedestrian-crossing scenario is simulated using Matlab R2020b. The map of the Scania test track is imported to Matlab and visualized in Fig. 5. A simple point-mass vehicle model is implemented for both the EV and CV, with each maintaining a constant velocity within their designated lanes. The headings of the EV and CV are determined based on the center points of their respective lanes. The EV, CV, and RSU are equipped with range-based sensors affected by random noise. These sensors are capable of producing measurement sets of the pedestrian with respect to their respective FOV and local coordinate system. These measurement sets include the uncertainty introduced by the random noise. These sensors generate measurement sets at a rate of 10 Hz, with the assumption that there is no delay in their operation. The CORA toolbox (Althoff, 2015) is utilized to handle constrained zonotopes. The ground truth location of the pedestrian is represented by a + sign.

5.1. Base scenario

For the occluded pedestrian-crossing scenario, four time instances

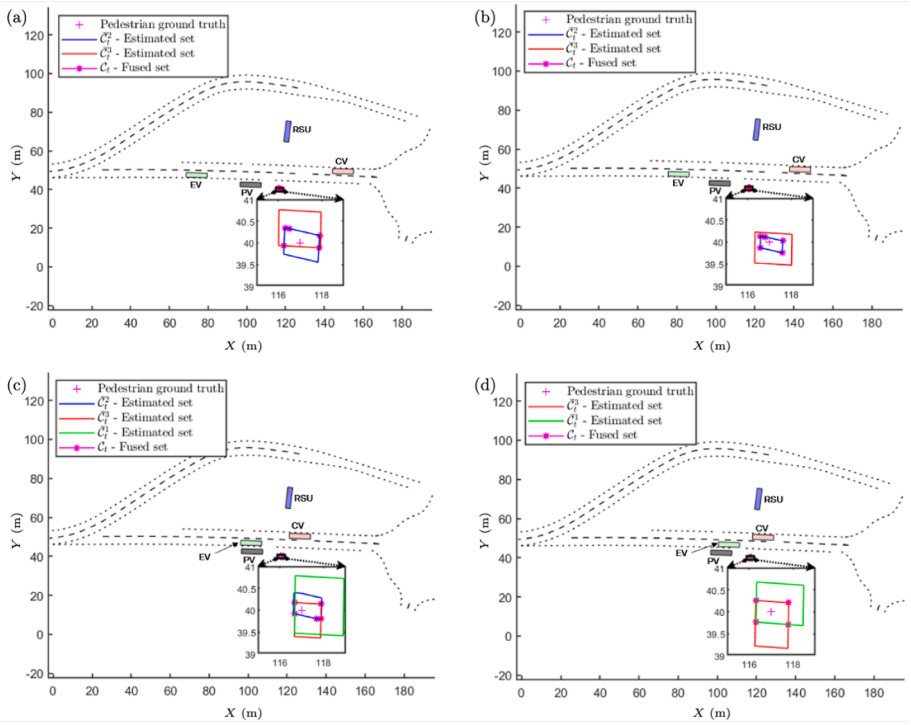

Fig. 5. Simulation of the occluded pedestrian-crossing scenario. Each sub-figure is a snapshot of the simulation at a specific time: (a) $t = 7.34$ s, (b) $t = 9.90$ s, (c) $t = 14.67$ s, and (d) $t = 15.48$ s. The + sign represents the true location of the pedestrian. The fused set $\mathscr{C}_t$ computed by Algorithm 1 is highlighted for the four time instances together with the estimated sets from each available sensor unit. Dashed lines represent roads.

are presented in Fig. 5. $\overline{\mathscr{C}}_t^1$ denote the estimated set computed based on the measurement set $\mathscr{M}_t^1$ obtained from the EV. Similarly, $\overline{\mathscr{C}}_t^2$ denote the estimated set based on the measurement set $\mathscr{M}_t^2$ obtained from the RSU and $\overline{\mathscr{C}}_t^3$ are the estimated set from the CV. In Figs. 5a and 5b, the EV does not have a measurement set for the pedestrian due to the occlusion created by the PV. In Fig. 5a, there are measurement sets from the RSU and CV. The estimated set computed using the measurement set from the RSU is represented by a blue constrained zonotope, while the estimated set computed using the measurement set from the CV is a red constrained zonotope. The resultant fused set $\mathscr{C}_t$ is a magenta constrained zonotope. Note that the pedestrian is located inside the fused set and that the set is a more accurate representation of the location than what the RSU and CV provided individually.

Fig. 5b presents a slighter later instance when still the pedestrian is not seen directly from the EV. The estimated sets $\overline{\mathscr{C}}_t^2$ and $\overline{\mathscr{C}}_t^3$ are smaller compared to Fig. 5a, as is the fused set $\mathscr{C}_t$. Fig. 5c shows a later instance when the pedestrian is detected also by the EV. Hence, in this case, there are three estimated sets fused into $\mathscr{C}_t$, which contains the pedestrian location. The fused set is tighter than any estimated set, as expected. Finally, Fig. 5d presents a case with the FOV of the RSU obstructed by the CV. Therefore, the RSU did not produce a measurement set. The fused set based on the estimated sets from the EV and CV contains the pedestrian's true location.

5.2. Influence of V2X communication

In this subsection, we analyze the occluded pedestrian-crossing scenario with and without V2X units, as well as with and without a pedestrian in the occluded region. The EV acts autonomously, and the system is designed to stop when safety cannot be guaranteed due to factors such as limited information caused by occlusion. Fig. 6 presents snapshots of the four scenario variations.

Fig. 6a presents the scenario with a pedestrian in the occluded region but no available V2X units. The pedestrian is approximately 15 m from the EV's front, but the EV is not able to detect the pedestrian. Therefore, the EV stops near the occlusion because of its limited situational awareness. The EV's velocities in x and y coordinates, respectively, are presented in the inset at left top of Fig. 6a. The EV stops at 14.03 s. The EV is unable to generate a feasible motion plan until it gathers more information about its surroundings.

In Fig. 6b, sensor information from two V2X units is available. These units are able to observe the pedestrian, and their measurement sets are shared with the EV. The EV can compute the fused set using the proposed method. The EV stops at 15.48 s to maintain a safe distance between itself and the detected pedestrian, and avoid the unsafe set. The safety distance is approximately 5 m from the front of the EV.

In Fig. 6c, there is no pedestrian in the occluded region and no available V2X units. Even if there is no pedestrian in the scenario, the EV has limited situational awareness, which leads to a stop near the occluded region. Hence, the consequence of no V2X units is a similar behavior for the EV as in Fig. 6a.

Fig. 6d presents the case when there is no pedestrian in the occluded region but two V2X units. Both sensors observe the occluded region, and implicitly communicate that the region is not occupied. As a result, the EV does not stop near the occlusion and operates at the desired velocity. It follows from the four cases illustrated in Fig. 6 that the overall performance of the EV is improved, thanks to the proposed situational awareness framework.

6. Experimental results

In this section, results from real experiments using Scania autonomous vehicles are discussed. Fig. 7 shows the picture taken from the EV's point-of-view during an experiment of the occluded pedestrian-crossing scenario. Fig. 7 includes a screen that displays the visualization tool used

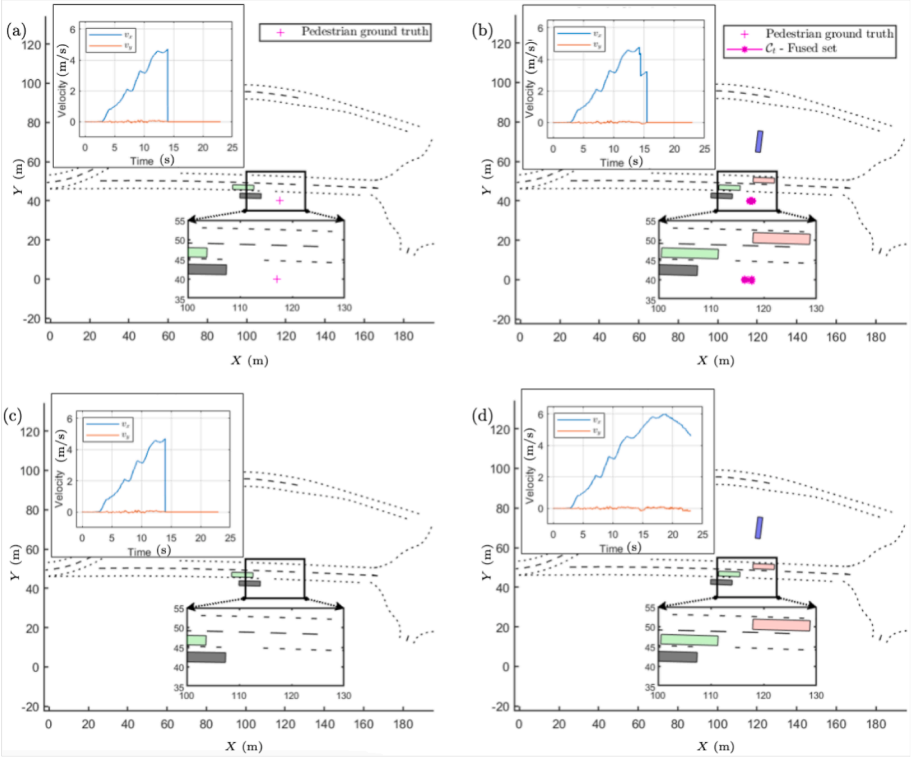

Fig. 6. Comparison of EV performance with and without V2X units, as well as with and without the pedestrian in the scenario. (a) Scenario with the pedestrian in the occluded region and without V2X units. (b) Scenario with the pedestrian in the occluded region and with V2X units. (c) Scenario without the pedestrian in the occluded region and without V2X units. (d) Scenario without the pedestrian in the occluded region and with V2X units.

during the experiments. The pedestrian is standing behind the parked vehicle and is not detected by the sensors mounted on the EV. This can be observed on the visualization tool, where the EV and PV positions are highlighted. A helicopter view of the experimental site is presented in Fig. 8, compared with Fig. 1. The EV, CV, and RSU are equipped with multiple sensors, such as, lidars and radars. The raw data from their respective sensors are then processed locally to produce measurement sets at a rate of 10 Hz. The processing time for each vehicle is approximately 200 ms. This processing time is taken into account in the measurement sets by proportionally increasing the associated uncertainty.

The V2X units communicate with EV using dedicated short-range communications (DSRC), built on the ITS-G5 standard. Similar to Wi-Fi, ITS-G5 is a European standard for vehicular communication based on IEEE 802.11x. The hardware utilized for this work is Commsignia ITS-OB4, the fourth generation of vehicular connectivity system. This hardware provides an embedded solution implementing the ITS-G5 access layer specification published by the European Telecommunications Standards Institute (ETSI), see ETSI (2020). The communication frequency is 5.9 GHz. The communication range varies depending on the operating area. In the scenario illustrated in Fig. 8, the communication range exceeds 1000 m due to the open-space setting and absence of obstructions such as buildings or other infrastructure. To be able to share measurement sets between the EV and V2X units, the collaborative perception message (CPM) service standard, see ETSI (2019), was implemented. The message frequency is 10 Hz and each message have an average payload of 100 B.

To analyze the communication delay, we recorded logs with GPS timestamps marking when a message was transmitted from one V2X unit and when it was received by the EV. Fig. 9 shows a graph of the communication delay between the EV and the V2X unit in an open-space setting. It can be observed that the average communication delay is about 0.02 s, which is negligible. Consequently, no compensation for communication delay was applied in the experiments.

Fig. 10 shows the snapshots from the occluded pedestrian-crossing scenario with connected RSU and CV sensor units. Fig. 10a the situation at $t = 2.05$ s. There are measurement sets from the RSU and CV. The estimated sets $\overline{\mathscr{C}}_t^2$ and $\overline{\mathscr{C}}_t^3$ are computed using Algorithm 1. The fused set $\mathscr{C}_t$ is shown as well. Fig. 10b shows the corresponding situation at $t = 6.47$ s is presented. It can be observed from Fig. 10 that the proposed framework successfully computed the fused sets from the V2X units and that the area of the fused sets is smaller than the two estimated sets.

Figs. 11a and 11b represent the computation time versus the product of number of constraints γ_c and number of generators e. Fig. 11a highlights the computation time for performing set-based estimation, where green, blue, and red highlights the computation time for estimating $\overline{\mathscr{C}}_t^1$, $\overline{\mathscr{C}}_t^2$, and $\overline{\mathscr{C}}_t^3$. It can be observed that the computation time increases as the number of constraints and generators increase, which validates the analysis of computational complexity in Section 4. Similarly, Fig. 11b shows the computation time for performing set-based fusion, where the magenta highlights the computation time to obtain $\mathscr{C}_t$. The computation time increases as the number of constraints and generators increase.

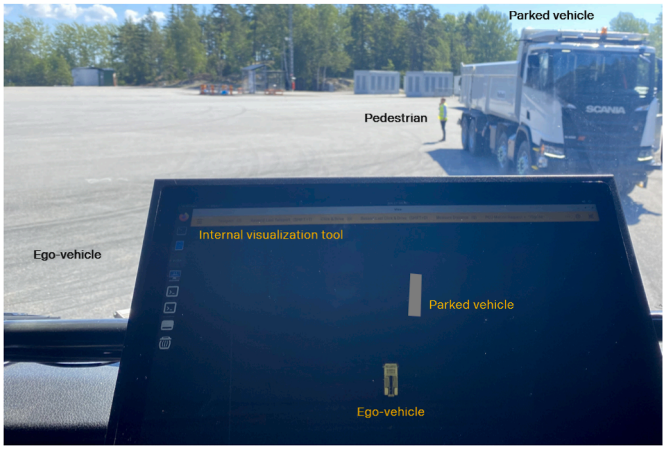

Fig. 7. View from the EV at an experiment showing the pedestrian behind the PV and the EV visualization tool.

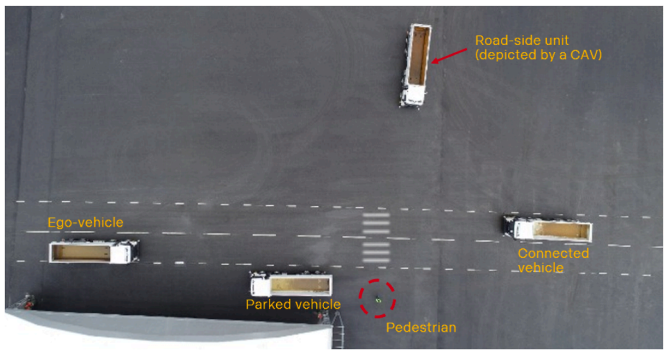

Fig. 8. Bird's-eye view of the Scania test track.

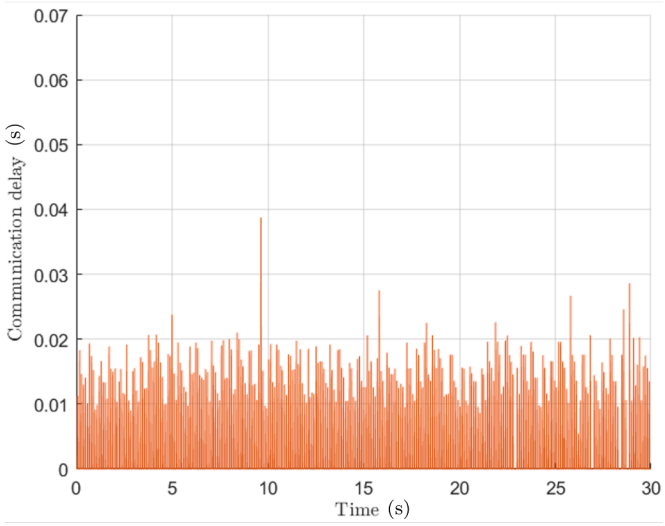

Fig. 9. Communication delay when communicating between EV and a V2X units in an open space scenario using dedicated short-range communication.

Fig. 12 shows experimental results with and without V2X units. In Fig. 12a, the understanding of the scene is based only on the local sensor information of the EV. There is an occluded region behind the parked vehicle and the building. In Fig. 12b, the RSU detects the pedestrian, and its measurement set is used to compute the estimated set $\overline{\mathscr{C}}_t^2$. In Fig. 12c, there are two V2X units, both the RSU and CV, providing measurement sets for the pedestrian. The corresponding $\mathscr{C}_t$ in this case is smaller than the previous two situations. Hence, V2X units help improve situational awareness by reducing the area and uncertainty of the unsafe set.

7. Conclusions

This study presented a set-based estimation and fusion algorithm for an occluded pedestrian-crossing scenario with safety guarantees. The method was implemented and illustrated both in simulation and in real experiments. Situational awareness of the EV with and without V2X communication was compared. It can be concluded that having V2X communication helps in improving the safety and performance of the EV.

While our method demonstrates strong performance under the

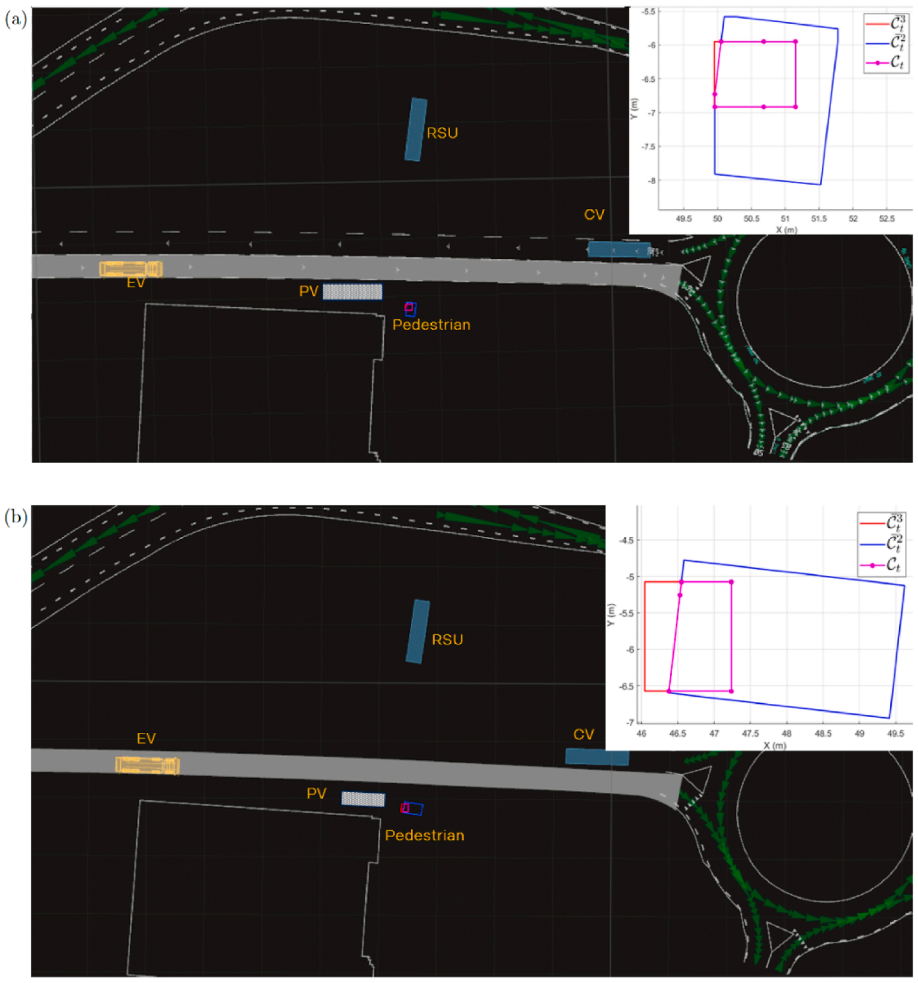

Fig. 10. Snapshots from experiments with estimated sets from the RSU and CV measurement sets at two time instance (a) $t = 2.05$ s and (b) $t = 6.47$ s.

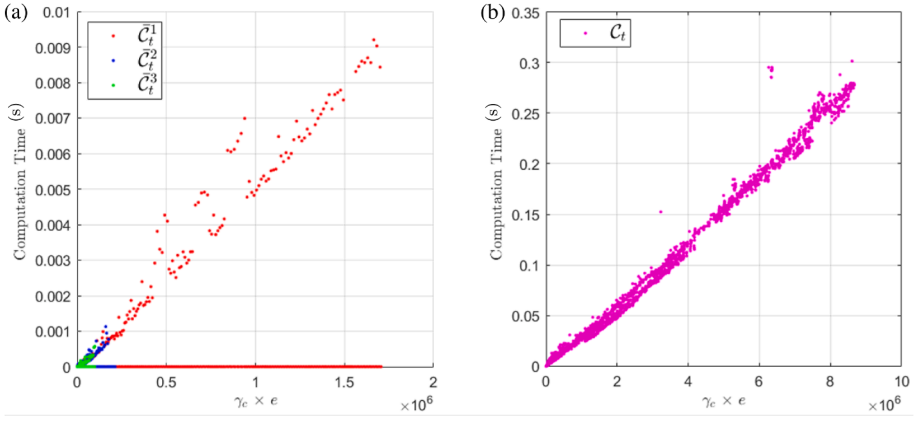

Fig. 11. Computation time versus product of number of constraints and number of generators for (a) set-based estimation and (b) set-based fusion. Note that in set-based estimation, the computation time is occasionally negligible. This occurs when only the predicted set is computed, as no measurement set is available.

experimental conditions outlined, we acknowledge that it is not without limitations. One key limitation is the system's sensitivity to false detections. Another potential failure case arises in scenarios involving multiple pedestrians in close proximity. By clarifying these aspects, we aim to provide a balanced perspective on the capabilities and constraints of our method, ensuring transparency and facilitating further work in this area. Future work includes handling more complex scenarios with multiple pedestrians and moving objects, as well as sensors and communication outages. The test scenario also needs to be included in an integrated framework for situational awareness.

CRediT authorship contribution statement

Vandana Narri: Writing – review & editing, Writing – original draft, Visualization, Resources, Methodology, Investigation, Formal analysis, Data curation, Conceptualization. **Amr Alanwar:** Writing – review &

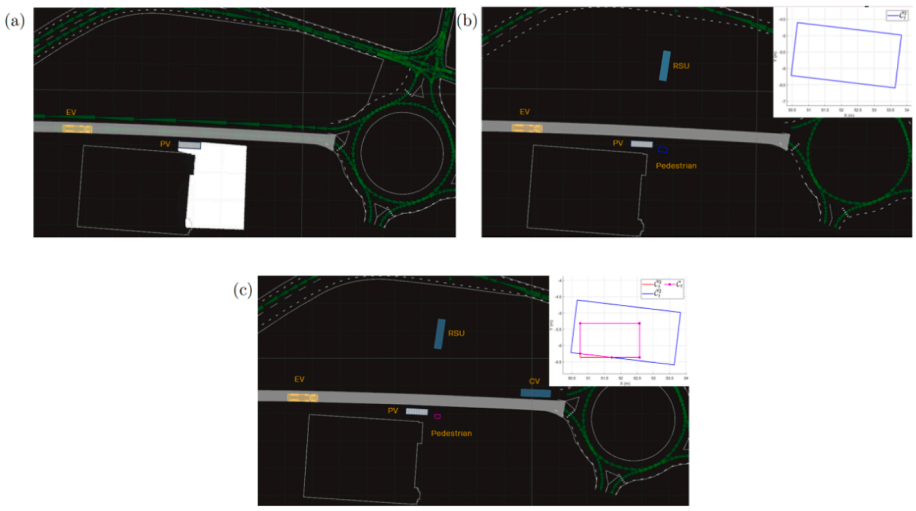

Fig. 12. Experiment results with pedestrian: (a) without V2X units, (b) with one V2X unit, and (c) with two V2X units.

editing, Supervision. **Jonas Mårtensson:** Writing – review & editing, Supervision, Conceptualization. **Henrik Pettersson:** Supervision, Resources, Data curation. **Fredrik Nordin:** Supervision, Investigation, Data curation. **Karl Henrik Johansson:** Writing – review & editing, Visualization, Supervision, Conceptualization.

Declaration of competing interest

The authors declare that they have no known competing financial interests or personal relationships that could have appeared to influence the work reported in this paper.

Acknowledgements

This work was partially supported by the Wallenberg Artificial Intelligence, Autonomous Systems, and Software Program (WASP) funded by the Knut and Alice Wallenberg Foundation. It was also partially supported by the Swedish Research Council Distinguished Professor (Grant No. 2017–01078) and the Knut and Alice Wallenberg Foundation Wallenberg Scholar Grant. We would like to thank Petter Wendel from Scania CV AB for his valuable insights and support.

References

Alanwar, A., Rath, J.J., Said, H., Johansson, K.H., Althoff, M., 2023. Distributed set-based observers using diffusion strategies. J. Franklin Inst. 360, 6976–6993.
Althoff, M., 2010. Reachability Analysis and its Application to the Safety Assessment of Autonomous Cars. Technische Universität München, München, Germany. Ph.D. Dissertation.
Althoff, M., 2015. An introduction to CORA 2015. In: Proceeding of the 1st and 2nd Workshop on Applied Verification for Continuous and Hybrid Systems: EasyChair, pp. 120–151.
Bento, L.C., Bonnifait, P., Nunes, U.J., 2019. Set-Membership position estimation with GNSS pseudorange error mitigation using lane-boundary measurements. IEEE Trans. Intell. Transport. Syst. 20, 185–194.
Blesa, J., Puig, V., Saludes, J., 2012. Robust fault detection using polytope-based set-membership consistency test. IET Control Theory & Appl. 6, 1767–1777.
Bouron, P., Meizel, D., Bonnifait, P., 2001. Set-membership non-linear observers with application to vehicle localisation. In: 2001 European Control Conference (ECC), pp. 1255–1260.
ETSI, 2019. Intelligent Transport Systems (ITS); Vehicular Communications; Basic Set of Applications; Analysis of the Collective Perception Service (CPS). https://www.etsi.org/.
ETSI, 2020. Intelligent Transport Systems (ITS); ITS-G5 Access Layer Specification for Intelligent Transport Systems Operating in the 5 GHz Frequency Band. https://www.etsi.org/.
Feng, X., Songlin, Y., Bin, L., 2020. Interval set-membership estimation for continuous linear systems. Int. J. Robust Nonlinear Control 30, 5305–5321.
Franzè, G., Lucia, W., 2015. The obstacle avoidance motion planning problem for autonomous vehicles: a low-demanding receding horizon control scheme. Syst. Control Lett. 77, 1–10.
García, R.A., Orihuela, L., Millan, P., Rubio, F.R., Ortega, M., 2020. Guaranteed estimation and distributed control of vehicle formations. Int. J. Control 93, 2729–2742.
Gilroy, S., Jones, E., Glavin, M., 2021. Overcoming occlusion in the automotive environment—a review. IEEE Trans. Intell. Transport. Syst. 22, 23–35.
Graebener, J.B.M., 2024. Formal Methods for Test and Evaluation: Reasoning over Tests, Automated Test Synthesis, and System Diagnostics. California Institute of Technology, Pasadena, USA. Ph.D. Dissertation.
Hamdi, S.E., Amairi, M., Aoun, M., 2016. Orthotopic set-membership parameter estimation of fractional order model. In: 2016 24th Mediterranean Conference on Control and Automation (MED), pp. 634–639.
Han, Y., Hui, Z., Huifang, L., Yi, J., Congyan, L., Yidong, L., 2023. Collaborative perception in autonomous driving: methods, datasets, and challenges. IEEE Intell Transp Syst Mag 15, 131–151.
Hieu, N., Hua, F., Honggang, W., 2023. Cooperative perception with V2V communication for autonomous vehicles. IEEE Trans. Veh. Technol. 72, 11122–11131.
ISO, 2022. ISO 21448:2022 Road Vehicles - Safety of the Intended Functionality. https://www.iso.org/standard/77490.html.
Jaulin, L., 2009. A nonlinear set membership approach for the localization and map building of underwater robots. IEEE Trans. Robot. 25, 88–98.
Jian, W., Yameng, S., Yuming, G., Rundong, Y., 2019. A survey of vehicle to everything (V2X) testing. Sensors (Peterb., NH) 19, 334.
Marco, M.D., Garulli, A., Giannitrapani, A., Vicino, A., 2003. Simultaneous localization and map building for a team of cooperating robots: a set membership approach. IEEE Trans. Robot. Autom. 19, 238–249.
Merhy, D., Maniu, C.S., Alamo, T., Camacho, E.F., Chabane, S.B., Chevet, T., et al., 2020. Guaranteed set-membership state estimation of an octorotor's position for radar applications. Int. J. Control 93, 2760–2770.
Monowar, H., Sibin, M., Takayuki, S., Hongsheng, L., 2020. Securing vehicle-to-everything (V2X) communication platforms. IEEE Trans. Intell. Veh. 5, 693–713.
Nyberg, T., Sánchez, J., Narri, V., Pettersson, H., Mårtensson, J., Johansson, K.H., et al., 2024. Share the unseen: sequential reasoning about occlusions using vehicle-to-everything technology. IEEE Trans. Control Syst. Technol. 1–14.
Olovsson, T., Svensson, T., Wu, J., 2022. Future connected vehicles: communications demands, privacy and cyber-security. Commun. Transp. Res. 2, 100056.
van der Ploeg, C., Nyberg, T., Sánchez, J., Silvas, E., van de Wouw, N., 2024. Overcoming fear of the unknown: occlusion-aware model-predictive planning for automated vehicles using risk fields. IEEE Trans. Intell. Transport. Syst. 25, 12591–12604.
Puig, V., 2010. Fault diagnosis and fault tolerant control using set-membership approaches: application to real case studies. Intern. J. Appl. Math. Comput. Sci. 20, 619–635.
Rego, B.S., Raimondo, D.M., Raffo, G.V., 2018. Set-based state estimation of nonlinear systems using constrained zonotopes and interval arithmetic. In: 2018 European Control Conference (ECC), pp. 1584–1589.
Rohou, S., Jaulin, L., Mihaylova, L., Le Bars, F., Veres, S.M., 2017. Guaranteed computation of robot trajectories. Robot. Autonom. Syst. 93, 76–84.
Ryan, Y., Ellick, C., Bin, C., Gaurav, B., 2018. Collaborative perception for automated vehicles leveraging vehicle-to-vehicle communications. In: 2018 IEEE Intelligent Vehicles Symposium (IV), pp. 1099–1106.
Scott, J.K., Raimondo, D.M., Marseglia, G.R., Braatz, R.D., 2016. Constrained zonotopes: a new tool for set-based estimation and fault detection. Automatica 69, 126–136.
Simon, U., Till, M., Andreas, R., Fabian, S., Markus, M., 2015. Defining and substantiating the terms scene, situation, and scenario for automated driving. In: 2015 IEEE 18th International Conference on Intelligent Transportation Systems, pp. 982–988.
Stefan, R., Thomas, P., Dieter, L., Bernhard, S., Frank, D., 2020. Survey on scenario-based safety assessment of automated vehicles. IEEE Access 8, 87456–87477.

Sánchez, J.M.G., Nyberg, T., Pek, C., Tumova, J., Törngren, M., 2022. Foresee the unseen: sequential reasoning about hidden obstacles for safe driving. In: 2022 IEEE Intelligent Vehicles Symposium (IV), pp. 255–264.
Wang, W., Wu, Y., 2021. Is uncertainty always bad for the performance of transportation systems? Commun. Transp. Res. 1, 100021.
Zhu, X., Jinmei, S., Hongbo, J., Geyong, M., Jinwen, L., Arun, I., 2024. Toward collaborative occlusion-free perception in connected autonomous vehicles. IEEE Trans. Mobile Comput. 23, 4918–4929.

Vandana Narri is currently pursuing the Ph.D. degree with a joint affiliation at Scania CV AB and the Division of Decision and Control Systems at KTH Royal Institute of Technology in Stockholm, Sweden. Her research aims to enhance situational awareness for heavy-duty vehicles in complex urban environments using vehicular communication and set-based methods. Her work is partially supported by the Wallenberg Artificial Intelligence, Autonomous Systems, and Software Program (WASP), funded by the Knut and Alice Wallenberg Foundation. She earned the M.S. degree in electrical engineering with a specialization in signal processing from Blekinge Institute of Technology, Karlskrona, Sweden in 2017.

Amr Alanwar is an Assistant Professor at Technical University of Munich, Germany, and an Adjunct Assistant Professor at Constructor University, Germany. He received the M.S. degree in computer engineering from Ain Shams University, Cairo, Egypt, in 2013 and the Ph.D. degree in computer science from the Technical University of Munich in 2020. He was a Postdoctoral Researcher at KTH Royal Institute of Technology. He was also a Research Assistant at the University of California, Los Angeles. He received the Best Demonstration Paper Award at the 16th ACM/IEEE International Conference on Information Processing in Sensor Networks (IPSN/CPSWeek 2017) and was a finalist in the Qualcomm Innovation Fellowship for two years in a row.

Jonas Mårtensson is a Professor in the Division of Decision and Control Systems at KTH Royal Institute of Technology. He serves as the Director of the Integrated Transport Research Lab (ITRL), a multidisciplinary research center focused on sustainable transport systems in collaboration with Swedish industry and public stakeholders. His research interests span efficient and sustainable transport systems, including cooperative traffic control and control of connected and automated vehicles, with a particular interest for freight and heavy vehicles. He received the M.S. degree in vehicle engineering in 2002 and the Ph.D. degree in automatic control in 2007, both from KTH Royal Institute of Technology. He was awarded the title of Docent in 2016.

Henrik Pettersson received the M.S. and Ph.D. degrees from the Division of Fluid and Mechanical Engineering Systems, Department of Mechanical Engineering at Linköping University, Linköping, Sweden, in 1995 and 2002, respectively. He began working for Scania CV AB in 2002, focusing on the development of powertrain control systems. Since 2010, he has worked in pre-development and research, concentrating on fuel-saving functionality for heavy-duty vehicles based on cooperative driving and V2X communication, such as platooning. Since 2016, his focus has shifted to autonomous vehicles. He is currently a senior technical advisor in the Autonomous Transport Solutions department at Scania CV AB.

Fredrik Nordin received the M.S. degree in computer engineering at the Luleå University of Technology in 2017. He began working as a development engineer with motion planning of autonomous vehicles at Scania CV AB in 2018 and has experience with implementing cooperative motion planning using V2X communication for confined areas. He is currently a research engineer focusing on solutions in the fields of situational awareness, motion planning and control for autonomous heavy vehicles designed for public road usage.

Karl Henrik Johansson is a Swedish Research Council Distinguished Professor in electrical engineering and computer science at KTH Royal Institute of Technology in Sweden and the Founding Director of Digital Futures. He earned the M.S. degree in electrical engineering and the Ph.D. degree in automatic control from Lund University. He has held visiting positions at UC Berkeley, Caltech, NTU, and other prestigious institutions. His research focuses on networked control systems and cyber-physical systems, with applications in transportation, energy, and automation networks. For his scientific contributions, he has received numerous best paper awards and distinctions from IEEE, IFAC, and other organizations. He has been recognized as a Distinguished Professor by the Swedish Research Council, a Wallenberg Scholar by the Knut and Alice Wallenberg Foundation, and a Future Research Leader by the Swedish Foundation for Strategic Research. He has also received the triennial IFAC Young Author Prize and the IEEE CSS Distinguished Lecturer award and is the recipient of the 2024 IEEE CSS Hendrik W. Bode Lecture Prize. His extensive service to the academic community includes roles as President of the European Control Association, IEEE CSS Vice President for Diversity, Outreach, and Development, and a member of the IEEE CSS Board of Governors and IFAC Council. He has served on the editorial boards of *Automatica*, *IEEE Transactions on Automatic Control*, *IEEE Transactions on Control of Network Systems*, etc. He has also been a Member of the Swedish Scientific Council for Natural Sciences and Engineering Sciences. He is a Fellow of both IEEE and the Royal Swedish Academy of Engineering Sciences.